Original Article | Neuroimaging and Head & Neck

eISSN 2005-8330
https://doi.org/10.3348/kjr.2023.1078
Korean J Radiol 2024;25(4):384-394

Korean Journal of Radiology
KJR

Dark-Blood Computed Tomography Angiography Combined With Deep Learning Reconstruction for Cervical Artery Wall Imaging in Takayasu Arteritis

Tong Su[1]*, Zhe Zhang[1]*, Yu Chen[1†], Yun Wang[1], Yumei Li[1], Min Xu[2], Jian Wang[2], Jing Li[3], Xinping Tian[3†], Zhengyu Jin[1]

[1]Department of Radiology, Peking Union Medical College Hospital, Chinese Academy of Medical Sciences & Peking Union Medical College, Beijing, China
[2]CT Business Unit, Canon Medical Systems (China), Beijing, China
[3]Department of Rheumatology and Clinical Immunology, Chinese Academy of Medical Sciences & Peking Union Medical College, National Clinical Research Center for Dermatologic and Immunologic Diseases (NCRC-DID), Ministry of Science & Technology, State Key Laboratory of Complex Severe and Rare Diseases, Peking Union Medical College Hospital (PUMCH), Key Laboratory of Rheumatology and Clinical Immunology, Ministry of Education, Beijing, China

Objective: To evaluate the image quality of novel dark-blood computed tomography angiography (CTA) imaging combined with deep learning reconstruction (DLR) compared to delayed-phase CTA images with hybrid iterative reconstruction (HIR), to visualize the cervical artery wall in patients with Takayasu arteritis (TAK).

Materials and Methods: This prospective study continuously recruited 53 patients with TAK (mean age: 33.8 ± 10.2 years; 49 females) between January and July 2022 who underwent head-neck CTA scans. The arterial- and delayed-phase images were reconstructed using HIR and DLR. Subtracted images of the arterial-phase from the delayed-phase were then added to the original delayed-phase using a denoising filter to generate the final-dark-blood images. Qualitative image quality scores and quantitative parameters were obtained and compared among the three groups of images: Delayed-HIR, Dark-blood-HIR, and Dark-blood-DLR.

Results: Compared to Delayed-HIR, Dark-blood-HIR images demonstrated higher qualitative scores in terms of vascular wall visualization and diagnostic confidence index (all $P < 0.001$). These qualitative scores further improved after applying DLR (Dark-blood-DLR compared to Dark-blood-HIR, all $P < 0.001$). Dark-blood DLR also showed higher scores for overall image noise than Dark-blood-HIR ($P < 0.001$). In the quantitative analysis, the contrast-to-noise ratio (CNR) values between the vessel wall and lumen for the bilateral common carotid arteries and brachiocephalic trunk were significantly higher on Dark-blood-HIR images than on Delayed-HIR images (all $P < 0.05$). The CNR values were significantly higher for Dark-blood-DLR than for Dark-blood-HIR in all cervical arteries (all $P < 0.001$).

Conclusion: Compared with Delayed-HIR CTA, the dark-blood method combined with DLR improved CTA image quality and enhanced visualization of the cervical artery wall in patients with TAK.

Keywords: Cervical artery, Takayasu arteritis; Computed tomography angiography; Deep learning; Artificial intelligence; Wall imaging

Received: October 30, 2023 **Revised:** January 25, 2024 **Accepted:** February 7, 2024

*†These authors contributed equally to this work.
Corresponding author: Yu Chen, MD, Department of Radiology, Peking Union Medical College Hospital, Chinese Academy of Medical Sciences & Peking Union Medical College, No.1 Shuaifuyuan, Dongcheng District, Beijing 100730, China
• E-mail: bjchenyu@126.com
Corresponding author: Xinping Tian, MD, Department of Rheumatology and Clinical Immunology, Chinese Academy of Medical Sciences & Peking Union Medical College, National Clinical Research Center for Dermatologic and Immunologic Diseases (NCRC-DID), Ministry of Science & Technology, State Key Laboratory of Complex Severe and Rare Diseases, Peking Union Medical College Hospital (PUMCH), Key Laboratory of Rheumatology and Clinical Immunology, Ministry of Education, No.1 Shuaifuyuan, Dongcheng District, Beijing 100730, China
• E-mail: tianxp6@126.com

Korean Journal of Radiology
KJR

INTRODUCTION

Takayasu arteritis (TAK) is a primary granulomatous large-vessel vasculitis that mostly affecting young women and leading to significant morbidity and mortality. It predominantly involves the large arteries, including the aorta, pulmonary artery, and their branches [1]. Carotid artery involvement is observed in 45%–84% of patients with TAK [2]. Prolonged disease can lead to various artery lesions such as arterial stenosis, occlusion, or aneurysmal dilation, which may result in symptoms of ischemic impairment such as limb pulselessness, mild headache, syncope, and stroke in patients with TAK [3]. Therefore, evaluation of carotid artery lesions is crucial for assessing TAK.

Computed tomography angiography (CTA) plays a vital role in the diagnosis of TAK, enabling evaluation of vessel involvement, quantitative assessment of disease activity, and treatment follow-up. Furthermore, CTA may reveal mural changes even in the early systemic phase when occlusive arterial changes are not evident [4]. Previous studies have reported distinctive mural changes in patients with TAK, such as circumferential wall thickening and enhancement, concentric low-attenuation ring, and circumferential calcification [5,6]. However, traditional bright-blood CTA images have limitations in observing the vessel wall because of the low contrast between the arterial wall and the lumen. Some advanced wall-imaging techniques based on the dark-blood protocol, such as turbo spin-echo MR that utilizes vascular flow void effects, can effectively depict abnormalities in vascular walls. This effect of blood signal suppression can also be realized by the way of CT post-processing techniques, including dual-energy CT material decomposition [7] and manual adjustment of CT value distribution [8]. In this study, we propose a new dark-blood CT method that utilizes a modified subtraction CT technique with reliable registration algorithms. We aimed to explore the feasibility of the dark-blood CT method for visualizing the carotid artery wall in patients with TAK.

In addition to dark-blood wall imaging, CT iterative reconstruction (IR) technology can help improve the image quality of vessel wall imaging. IR, especially hybrid IR (HIR) processed in both the image and raw-data domain has been widely used in daily practice. HIR offers an overall improvement in image quality compared to the previous filtered back projection and does not suffer from the high computational time issue of model-based IR (MBIR). However, some studies have reported limitations in low-contrast lesion detectability and spatial resolution when using HIR methods [9]. Recently, deep learning reconstruction (DLR) [10] based on convolutional neural networks (CNNs) was proposed to further enhance the spatial resolution and diagnostic performance without affecting the noise texture. Previous studies demonstrated the benefits of DLR on coronary CT angiography [11-14], abdominal contrast-enhanced dual-energy CT [15], and brain CTA [16]. Here, we have extended the application of the DLR algorithm to dark-blood CTA to evaluate vessel wall imaging in the head and neck region.

The purpose of this study was to assess the image quality of a newly developed dark-blood CTA imaging technique combined with DLR in visualizing the cervical artery wall of patients with TAK, compared to delayed-phase CTA images with HIR.

MATERIALS AND METHODS

Study Patients

This prospective study was approved by the ethics committee of our institution (IRB No. I-24PJ0479). Written informed consent was obtained from all the patients. Fifty-three patients (4 males; mean age, 33.8 ± 10.2 years; range, 17–66 years) were consecutively recruited from January 2022 to July 2022. All patients underwent head-neck CTA at our institution. The inclusion criteria were as follows: 1) clinical diagnosis of TAK and 2) suspicion of cervical artery involvement. The exclusion criteria were as follows: 1) contraindications for CTA scanning, 2) history of carotid vascular graft surgery, and 3) limited observation of the cervical arteries due to obvious artifacts caused by metal implants, such as internal fixation surgery of the cervical vertebrae and extensive dental implants.

CT Acquisition

All scans were performed using a 320-row-detector CT scanner (Aquilion ONE Genesis Edition, Canon Medical Systems, Otawara, Japan). Patients were positioned supine with their arms placed at their sides and instructed not to move their heads during the examination.

The scan range was from the aortic arch to the skull. The monitoring trigger for the contrast scan was positioned at the level of the thoracic aorta with a threshold value of 180 Hounsfield unit. A high-pressure syringe with a double cylinder was used to inject 55 mL of the contrast agent, Ultravist (370 mg I/mL), and 25 mL of

 https://doi.org/10.3348/kjr.2023.1078

saline at a rate of 4 mL/s through the right median cubital vein. Bolus tracking was triggered to start the arterial-phase scanning. Delayed-phase imaging was performed 90 s after contrast medium injection. The scanning parameters were as follows: tube voltage 100 kVp, intelligently and automatically modulated tube current, rotational speed 0.5 s/r, the noise index (standard deviation [SD]) set to 7.5, display-field of view (D-FOV) 300 (M), collimation of 0.5 x 160, matrix size of 512 x 512, and pitch of 0.8.

The CT dose index volume (CTDIvol; mGy) and dose-length product (DLP; mGy·cm) were recorded from the CT scanner. The effective radiation dose (mSv) was calculated as the product of the DLP and a conversion factor of 0.0048 mSv/(mGy·cm) for craniocervical CTA [17].

Image Reconstruction and Post-Processing

The DLR algorithm (Advanced Intelligent Clear-IQ Engine, AiCE, Canon Medical Systems) used in this study was developed by introducing CNNs trained with high-quality target images generated using MBIR. This training process consisted of iteratively repeating the input-forward, error-backpropagation operation, achieving all the benefits of MBIR and thus turning low-quality input data into high-quality images that were free of noise contamination [18]. Arterial and delayed-phase images were reconstructed using HIR (Adaptive Iterative Dose Reduction [AIDR] 3D, FC03, Canon Medical Systems) and DLR (AiCE, body sharp kernel, Canon Medical Systems), with a slice thickness of 1.0 mm and an interval of 1.0 mm. Subsequently, these two groups of images with the same reconstruction algorithm were sent to dedicated post-processing software (^{SURE}Subtraction, Canon Medical Systems) to generate dark-blood CT images. This process consisted of two steps: first, subtraction images were obtained by subtracting arterial-phase CT images from delayed-phase CT images; then, subtraction images were added to the original delayed-phase images using an automatic denoising procedure to generate the final dark-blood CT images (Fig. 1). Therefore, three groups of CTA images were produced for analysis: Delayed-HIR, Dark-blood-HIR, and Dark-blood-DLR.

Image Analysis

Qualitative Image Quality Analysis

Qualitative image quality was independently rated by two experienced radiologists (T.S. and Z.Z.) with 7- and 5-year experience in head-neck angiography imaging, respectively. The items were rated on a five-point Likert

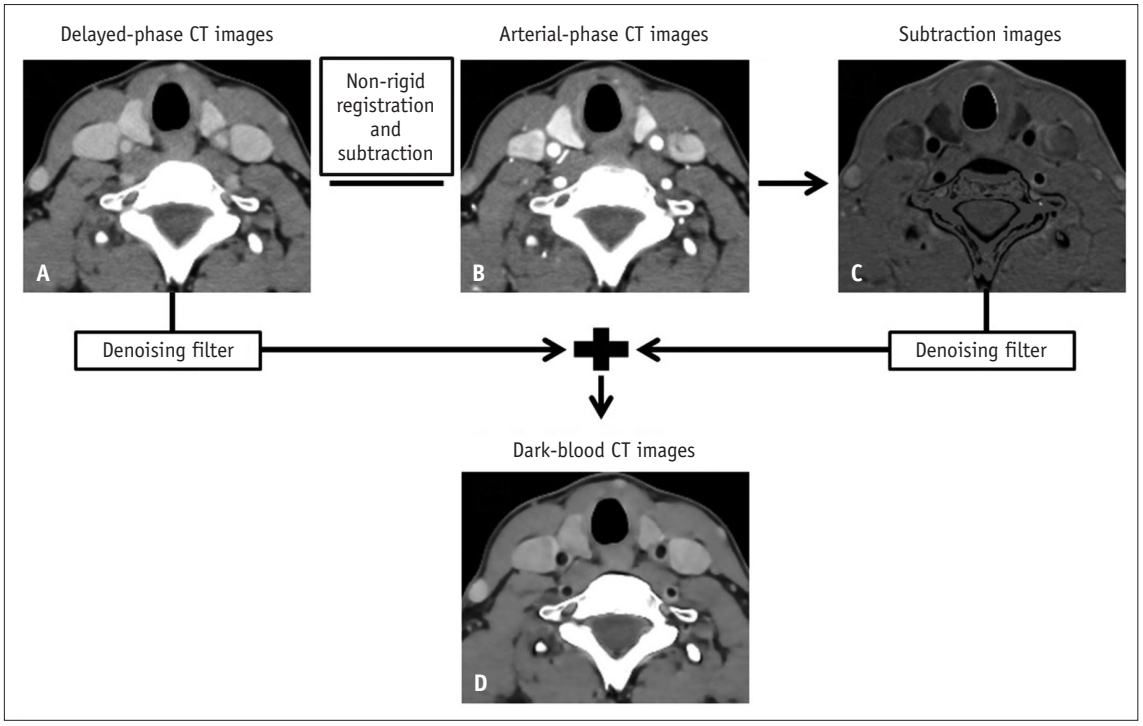

Fig. 1. Principles of the dark-blood CTA technique. **A-C:** The subtraction image **(C)** is obtained by subtracting the arterial-phase CT image **(B)** from the delayed-phase image **(A)**. Dark-blood CT images **(D)** are obtained by adding delayed-phase images to subtraction images using a denoising filter, and clearly display the arterial vessel wall. CTA = computed tomography angiography

https://doi.org/10.3348/kjr.2023.1078

Korean Journal of Radiology
KJR

scale. Images from the three CT image sets were randomly arranged and reviewed after blinding patient information. Although the imaging methods were not revealed to the readers, strict blinding of the imaging methods was not feasible owing to their intrinsic differences. The qualitative evaluation included the following criteria: overall image noise (1 = too much noise to evaluate, 2 = too much noise, only the tissue contour can be evaluated, 3 = acceptable noise, morphology and density can be evaluated, 4 = less noise, accurate diagnosis can be evaluated, and 5 = very little noise, accurate diagnosis can be quickly evaluated); ability of vessel wall visualization (1 = unable to judge whether the vessel wall is thickened, 2 = whether the vessel wall is thickened can be evaluated, but cannot be measured accurately, 3 = vessel wall thickness can be measured, 4 = vessel wall thickness can be measured accurately, and 5 = vessel wall thickness can be measured quickly and accurately); and diagnostic confidence index (1 = no confidence to diagnose, 2 = no confidence to ensure accurate measurements, 3 = accurate measurements can be ensured, 4 = full confidence in diagnosis, and 5 = diagnosis is ensured quickly and accurately). Higher scores indicated better image quality.

Quantitative Image Quality Analysis

All CT images were manually segmented by an experienced radiologist (T.S.) with 7-year experience in head-neck angiography imaging using the open-source software ITK-SNAP (http://www.itksnap.org/pmwiki/pmwiki.php). On CTA images of each patient, five cervical arteries (brachiocephalic trunk, bilateral subclavian arteries, and common carotid arteries) were selected and one region of interest (ROI) was drawn for each. The slice with the thickest vessel wall was identified, and three concentric ROIs were drawn for each artery to represent the characteristics of the thickened vessel wall. The smallest ROI was placed within the vessel lumen, the middle ROI was drawn along the inner edge of the vessel wall, and the largest ROI was drawn along the outer edge of the vessel wall. Arteries that were convoluted, interfered with venous contrast agent artifacts, or lacked closed circular structures on the axial image were excluded from the analysis. This was commonly observed in the brachiocephalic trunk and bilateral subclavian arteries. Arteries with occluded vascular lumen or stent implantation were excluded from the analysis. The shape, size, and location of the ROIs were kept the same for the three datasets using copy and paste commands.

Python version 3.6.4 (https://www.python.org) was used to compute quantitative parameters, including density, SD, signal-to-noise ratio (SNR), and contrast-to-noise ratio (CNR). The SNR of the vessel wall and the CNR between the vessel wall and lumen are defined as follows:

$$SNR = \frac{Density_{wall}}{SD_{wall}}$$

$$CNR = \frac{|\ Density_{wall} - Density_{lumen}\ |}{\sqrt{\frac{1}{2}(SD^2_{wall} + SD^2_{lumen})}}$$

Vessel Wall Thickness Measurement

The wall thickness of the common carotid artery was independently measured by two experienced radiologists (T.S. and Z.Z.) with 7- and 5-year experience in head-neck angiography imaging, respectively. Measurements were taken at the thickest layer of the common carotid artery wall in three groups of CTA images.

Statistical Analysis

Statistical analyses were conducted using R software (version 3.6.1; http://www.R-project.org). The Shapiro–Wilk test was used to assess the normal distribution of the data. If the data were normally distributed, a one-way repeated measures ANOVA was employed to analyze the differences among multiple groups. For multiple comparisons, paired sample *t*-tests with Bonferroni correction for *P*-values were applied. In cases where the data did not follow a normal distribution, the Friedman test was used to analyze the differences among multiple groups. Additionally, the Wilcoxon signed-rank test with the Bonferroni correction of *P*-values was performed for multiple comparisons. Statistical significance was set at $P < 0.05$. Kappa statistics were used to assess inter-rater agreement between the two readers for qualitative evaluation. A kappa value greater than 0.75 was considered excellent, between 0.40 and 0.75 was considered fair to good, while value less than 0.40 was regarded as poor. Inter-rater variability was evaluated using the intraclass correlation coefficient (ICC) for vessel wall thickness measurements. ICC values less than 0.4, between 0.4 and 0.75, and greater than 0.75 were interpreted as representing poor agreement, good agreement, and excellent agreement, respectively.

https://doi.org/10.3348/kjr.2023.1078

RESULTS

Participants and Radiation Dose

A total of 53 patients were enrolled in this study; 92.4% were females with a mean age of 33.8 years. A total of 182 ROIs were obtained from the following locations: the brachiocephalic trunk (n = 31), left subclavian arteries (n = 34), right subclavian arteries (n = 19), left common carotid arteries (n = 48), and right common carotid arteries (n = 50). The patient inclusion flowchart is shown in Figure 2.

The CTDIvol, DLP, and effective radiation dose for the non-enhanced phase were 11.24 ± 1.49 mGy, 496.93 ± 65.09 mGy·cm, and 2.39 ± 0.31 mSv, respectively. The CTDIvol, DLP, and effective radiation dose for the arterial-phase were 15.16 ± 1.99 mGy, 670.33 ± 87.11 mGy·cm, and 3.22 ± 0.42 mSv, respectively. The CTDIvol, DLP, and effective radiation dose for the delayed-phase were 15.16 ± 1.99 mGy, 670.33 ± 87.11 mGy·cm, and -3.22 ± 0.42 mSv, respectively.

Qualitative Evaluation of Image Quality

The qualitative evaluation scores are listed in Table 1. When compared with Delayed-HIR images, CTA images processed using the dark-blood technique presented higher qualitative scores in terms of vascular wall visualization and diagnostic confidence index (all $P < 0.05$). In terms of overall image noise, Dark-blood-HIR scores were comparable to Delayed-HIR scores (all $P > 0.05$). The qualitative scores of Dark-blood-HIR for overall image noise, vascular wall visualization, and diagnostic confidence index were further increased with DLR (all $P < 0.05$). Figures 3 and 4 present two representative examples of Delayed-HIR, Dark-blood-HIR, and Dark-blood-DLR images. These were taken at varying levels of the common carotid and subclavian arteries in two patients with TAK. In both cases, the Dark-blood-DLR images provide improved visualization of the artery wall structure.

For overall image noise, vessel wall visualization ability, and diagnostic confidence index, the two raters showed excellent agreement, with kappa values of 0.829, 0.848, and 0.867, respectively.

Quantitative Evaluation of Image Quality

The SNRs of the five cervical arteries of the Dark-blood-HIR images were comparable to those of the Delayed-HIR images (all $P > 0.05$, Table 2). The SNRs of the Dark-

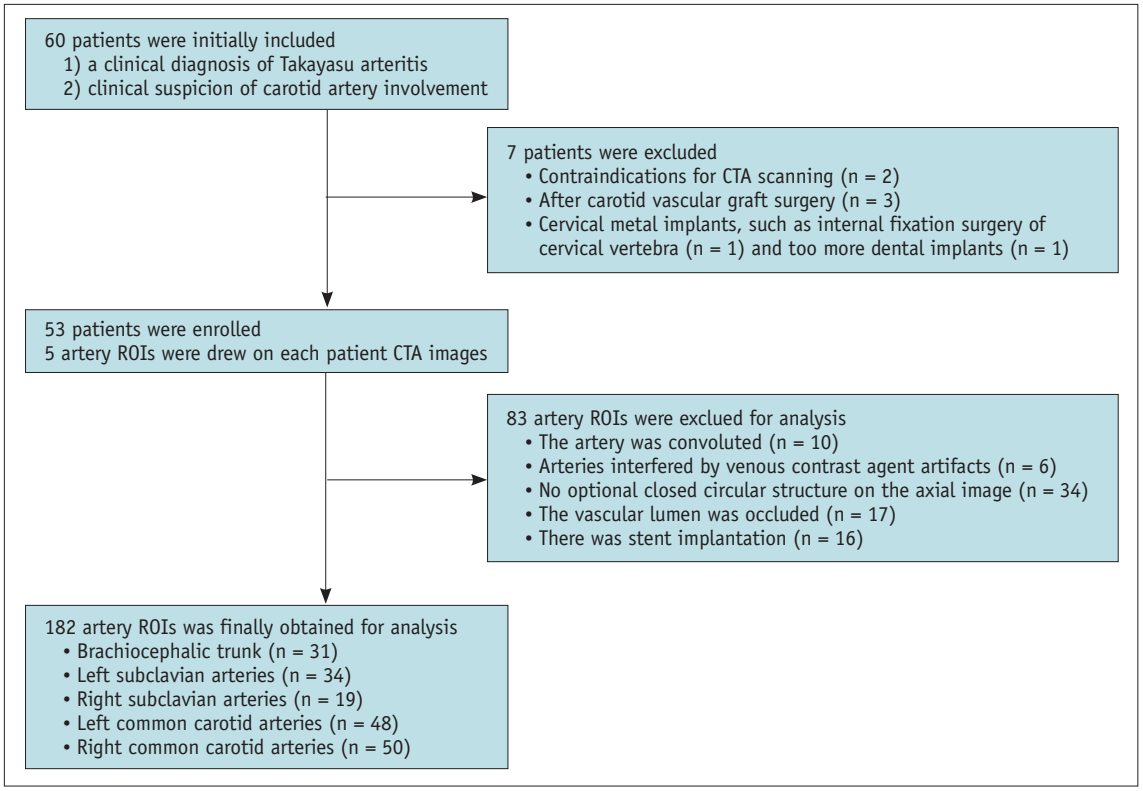

Fig. 2. Flow chart of patient enrollment and study design. Based on the predefined inclusion and exclusion criteria, 53 patients successfully underwent head-neck CTA. CTA = computed tomography angiography, ROI = region of interest

https://doi.org/10.3348/kjr.2023.1078

Korean Journal of Radiology
KJR

blood-DLR images were significantly higher for the five cervical arteries than those of the Dark-blood-HIR images (all $P < 0.01$, Table 2). The CNRs of Dark-blood-HIR were significantly higher than those of Delayed-HIR for the left common carotid artery, right common carotid artery, and brachiocephalic trunk (all $P < 0.05$). The CNRs of all five cervical arteries of the Dark-blood-DLR images were significantly higher than those of the Dark-blood-HIR images

Table 1. Qualitative image quality scores of Delayed-HIR, Dark-blood-HIR, and Dark-blood-DLR images

Parameter and reader	n	Image quality score			*P*			
		Delayed-HIR (group 1)	Dark-blood-HIR (group 2)	Dark-blood-DLR (group 3)	All	1 vs. 2	2 vs. 3	1 vs. 3
Overall image noise	53							
Reader 1		4.0 ± 0.3	3.9 ± 0.3	4.9 ± 0.2	< 0.001	1.000	< 0.001	< 0.001
Reader 2		3.8 ± 0.4	3.9 ± 0.4	4.9 ± 0.3	< 0.001	0.110	< 0.001	< 0.001
Vessel wall visualization	53							
Reader 1		2.9 ± 0.7	3.8 ± 0.7	4.8 ± 0.5	< 0.001	< 0.001	< 0.001	< 0.001
Reader 2		2.8 ± 0.7	3.8 ± 0.7	4.7 ± 0.5	< 0.001	< 0.001	< 0.001	< 0.001
Diagnostic confidence index	53							
Reader 1		2.9 ± 0.8	3.8 ± 0.8	4.7 ± 0.6	< 0.001	< 0.001	< 0.001	< 0.001
Reader 2		2.7 ± 0.7	3.8 ± 0.6	4.7 ± 0.6	< 0.001	< 0.001	< 0.001	< 0.001

Data are mean ± standard deviation. The *P*-values for multiple pairwise comparisons were adjusted using Bonferroni method, and $P < 0.05$ indicates statistically significant difference.
HIR = hybrid iterative reconstruction, DLR = deep learning reconstruction

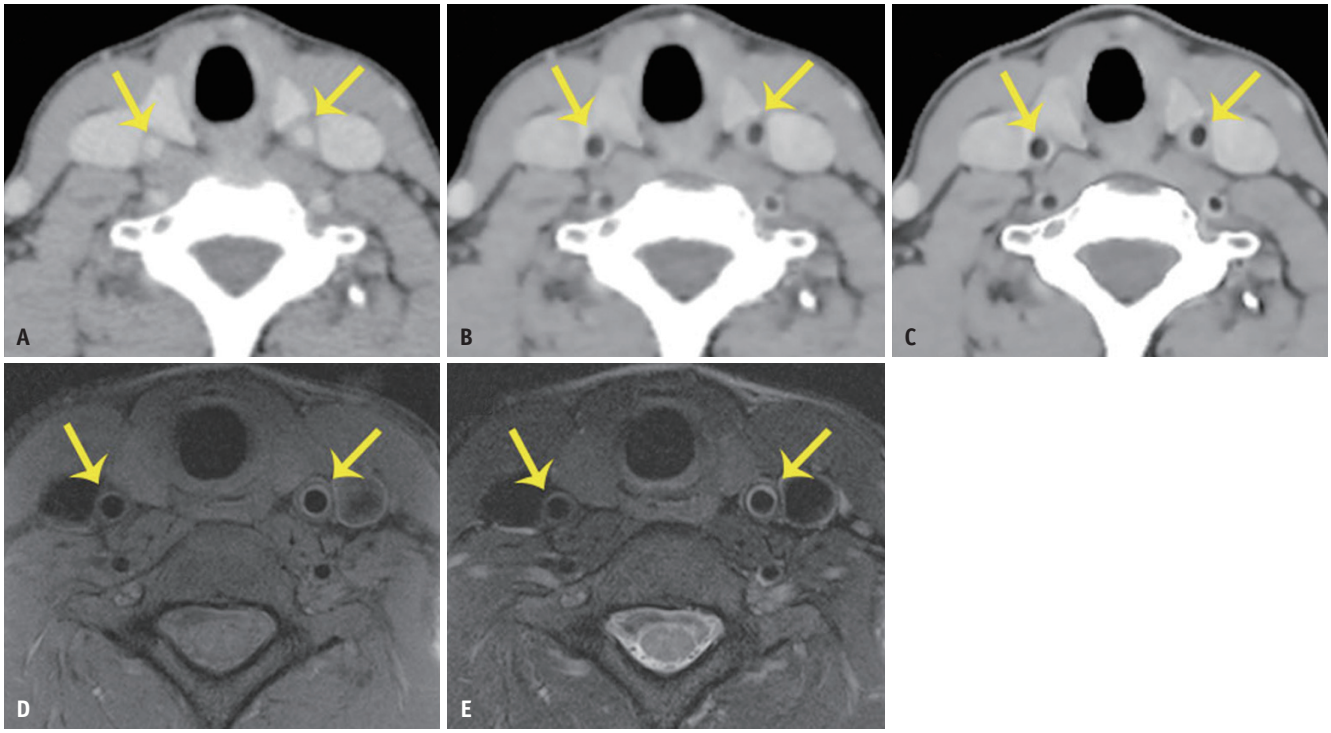

Fig. 3. An illustrative case of a 35-year-old female with Takayasu arteritis. **A-E:** CTA images **(A-C)** and carotid artery vessel wall MRI images **(D-E)** reveal thickening of bilateral common carotid arteries (arrows). Compared to Delayed-HIR **(A)**, CTA images using the dark-blood method **(B)** show enhancement of the vascular wall visualization and diagnostic confidence index for thickened carotid artery vessel walls. In addition, dark-blood CTA images combined with DLR **(C)** yield better overall image quality with reduced image noise and display the highest contrast-to-noise ratio value between the vessel wall and lumen. The thickened vessel walls of bilateral common carotid arteries (arrows) show hyper/iso-intensity on T2WI **(D)** and iso-intensity on T1WI **(E)** of MRI obtained outside the research protocol. CTA = computed tomography angiography, MRI = magnetic resonance imaging, HIR = hybrid iterative reconstruction, DLR = deep learning reconstruction, WI = weighted imaging

https://doi.org/10.3348/kjr.2023.1078

(all $P < 0.001$, Table 2).

Except for the right common carotid artery, the mean density and SD values of the other four arterial walls of the Dark-blood-HIR images were comparable to those of the Delayed-HIR images (all $P > 0.05$, Table 3). Dark-blood-DLR significantly increased the mean density and decreased

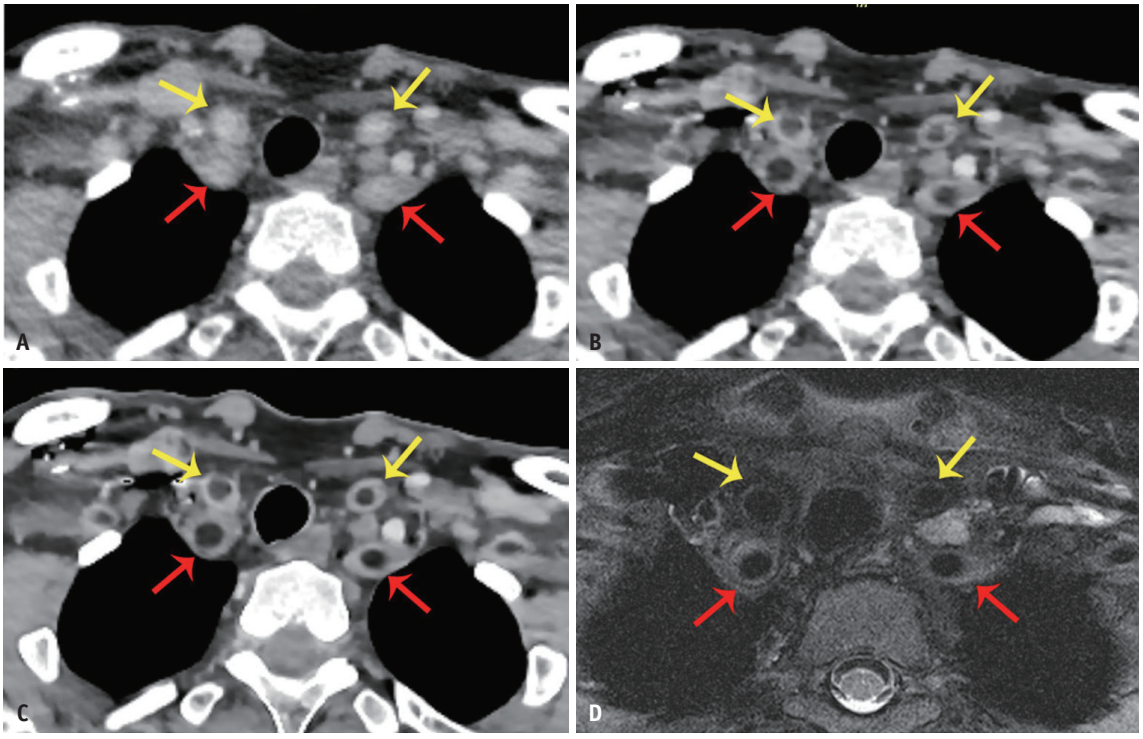

Fig. 4. An illustrative case of a 34-year-old female with Takayasu arteritis. **A-D:** CTA images **(A-C)** and carotid artery vessel wall MRI images **(D)** exhibit thickening of bilateral common carotid arteries (yellow arrows) and subclavian artery (red arrows) at the level of the lower neck. Compared to Delayed-HIR **(A)**, CTA images using the dark-blood method **(B)** display enhancement of vascular wall visualization and diagnostic confidence index for the thickened artery vessel wall. Furthermore, dark-blood CTA images combined with DLR **(C)** result in overall image quality improvement with reduced image noise and the highest contrast-to-noise ratio value between the vessel wall and lumen. The thickened vessel walls of the common carotid arteries (yellow arrows) and subclavian artery (red arrows) show hyper/iso-intensity on T2WI **(D)** obtained outside the research protocol. CTA = computed tomography angiography, MRI = magnetic resonance imaging, HIR = hybrid iterative reconstruction, DLR = deep learning reconstruction, WI = weighted imaging

Table 2. SNRs and CNRs of Delayed-HIR, Dark-blood-HIR, Dark-blood-DLR images

Parameter and vessel	n	Quantitative values			*P*			
		Delayed-HIR (group 1)	Dark-blood-HIR (group 2)	Dark-blood-DLR (group 3)	All	1 vs. 2	2 vs. 3	1 vs. 3
SNR								
Brachiocephalic trunk	31	2.2 ± 0.8	2.3 ± 0.9	2.8 ± 1.1	< 0.001	0.271	< 0.001	< 0.001
Left subclavian artery	34	1.9 ± 0.6	1.7 ± 0.8	2.5 ± 0.9	< 0.001	0.572	< 0.001	< 0.001
Right subclavian artery	19	1.4 ± 0.8	1.6 ± 0.8	2.3 ± 1.0	< 0.001	0.110	< 0.001	< 0.001
Left common carotid artery	48	3.4 ± 1.7	3.6 ± 1.9	3.9 ± 1.9	0.005	1.000	0.011	0.008
Right common carotid artery	50	3.7 ± 1.4	3.7 ± 1.7	4.0 ± 2.0	0.038	1.000	0.003	0.111
CNR between the vascular wall and lumen								
Brachiocephalic trunk	31	2.6 ± 1.0	3.6 ± 1.7	4.9 ± 1.8	< 0.001	0.009	< 0.001	< 0.001
Left subclavian artery	34	2.7 ± 0.8	2.7 ± 1.2	4.9 ± 2.1	< 0.001	1.000	< 0.001	< 0.001
Right subclavian artery	19	2.3 ± 0.8	2.6 ± 1.5	4.1 ± 1.0	< 0.001	1.000	< 0.001	0.001
Left common carotid artery	48	3.8 ± 1.3	5.1 ± 3.1	7.2 ± 4.1	< 0.001	0.009	< 0.001	< 0.001
Right common carotid artery	50	3.3 ± 1.1	5.2 ± 2.4	6.6 ± 2.6	< 0.001	< 0.001	< 0.001	< 0.001

Data are mean ± standard deviation. The *P*-values for multiple pairwise comparisons were adjusted using Bonferroni method, and $P < 0.05$ indicates statistically significant difference.
SNR = signal-to-noise ratio, CNR = contrast-to-noise ratio, HIR = hybrid iterative reconstruction, DLR = deep learning reconstruction

https://doi.org/10.3348/kjr.2023.1078

Korean Journal of Radiology
KJR

the SD values of all cervical artery walls compared to Dark-blood-HIR images (Table 3). For the vessel lumen, the dark-blood technique significantly reduced the mean density of all cervical arteries compared to Delayed-HIR images (all $P < 0.001$, Table 3) and significantly reduced the SD values of the vessel lumen of the bilateral common carotid arteries (left, $P < 0.001$; right, $P = 0.01$; Table 3). The mean density and SD values of all cervical arteries of the Dark-blood-DLR group were further reduced compared to those of the Dark-blood-HIR group (all $P < 0.006$, Table 3).

Measurements of Vessel Wall Thickness

The vessel wall thickness of common carotid arteries were 1.98 ± 0.76 mm, 2.25 ± 0.76 mm and 2.19 ± 0.70 mm measured by reader 1 on Delayed-HIR, Dark-blood-HIR, and Dark-blood-DLR images respectively. By reader 2, the vessel wall thickness of common carotid arteries were measured as 2.29 ± 0.71 mm, 2.48 ± 0.86 mm and 2.33 ± 0.80 mm on Delayed-HIR, Dark-blood-HIR, and Dark-blood-DLR images respectively. The ICC values between the two readers were 0.903 (0.836, 0.943), 0.896 (0.825, 0.939) and 0.958 (0.927, 0.976) for Delayed-HIR, Dark-blood-HIR, and Dark-blood-DLR images respectively. The highest ICC value between the two raters was observed for the Dark-blood-DLR images.

DISCUSSION

In this study, a novel subtraction-based dark-blood CT imaging technique combined with DLR was investigated, and its application was evaluated in the imaging of the cervical arterial wall in patients with TAK. The findings indicate that dark-blood CTA images allowed better visualization of arterial walls compared to the Delayed-HIR technique. Furthermore, the combination of dark-blood imaging with DLR resulted in additional enhancement of

Table 3. CT attenuation and noise of Delayed-HIR, Dark-blood-HIR, and Dark-blood-DLR images

Parameters	n	Quantitative values			*P*			
		Delayed-HIR (group 1)	Dark-blood-HIR (group 2)	Dark-blood-DLR (group 3)	All	1 vs. 2	2 vs. 3	1 vs. 3
Delayed-HIR (group 1) CT attenuation of vascular wall (HU)								
Brachiocephalic trunk	31	62.4 ± 15.9	67.4 ± 18.5	74.1 ± 18.1	< 0.001	0.094	< 0.001	< 0.001
Left subclavian artery	34	57.7 ± 15.8	55.7 ± 20.3	72.8 ± 21.3	< 0.001	0.876	< 0.001	< 0.001
Right subclavian artery	19	50.0 ± 20.3	51.9 ± 21.4	64.9 ± 19.7	< 0.001	1.000	< 0.001	0.002
Left common carotid artery	48	70.6 ± 20.4	68.5 ± 19.4	79.8 ± 17.6	< 0.001	0.230	< 0.001	< 0.001
Right common carotid artery	50	79.1 ± 17.9	72.0 ± 21.2	81.8 ± 21.0	< 0.001	< 0.001	< 0.001	0.175
CT attenuation of lumen (HU)								
Brachiocephalic trunk	31	100.1 ± 41.4	-13.3 ± 46.7	-29.4 ± 30.0	< 0.001	< 0.001	< 0.001	< 0.001
Left subclavian artery	34	120.9 ± 26.4	-9.8 ± 38.5	-37.1 ± 35.1	< 0.001	< 0.001	< 0.001	< 0.001
Right subclavian artery	19	113.1 ± 29.8	-8.5 ± 53.1	-21.4 ± 36.4	< 0.001	< 0.001	< 0.001	0.002
Left common carotid artery	48	132.8 ± 30.5	-7.4 ± 46.6	-34.7 ± 41.8	< 0.001	< 0.001	< 0.001	< 0.001
Right common carotid artery	50	134.1 ± 26.1	-8.1 ± 47.4	-26.2 ± 36.9	< 0.001	< 0.001	< 0.001	< 0.001
Image noise of vascular wall (HU)								
Brachiocephalic trunk	31	30.0 ± 7.2	31.3 ± 11.3	29.4 ± 10.7	0.078	1.000	0.045	0.472
Left subclavian artery	34	32.5 ± 6.9	33.9 ± 9.9	31.6 ± 9.4	0.187	1.000	0.160	0.640
Right subclavian artery	19	39.6 ± 12.1	36.6 ± 13.3	30.4 ± 9.1	< 0.001	0.219	0.021	0.002
Left common carotid artery	48	22.7 ± 6.2	22.4 ± 7.4	23.9 ± 8.4	0.012	0.589	0.008	0.578
Right common carotid artery	50	23.3 ± 6.2	21.8 ± 5.9	23.4 ± 7.4	0.003	0.020	0.004	1.000
Image noise of lumen (HU)								
Brachiocephalic trunk	31	16.7 ± 5.4	17.4 ± 8.5	10.6 ± 4.2	< 0.001	1.000	< 0.001	< 0.001
Left subclavian artery	34	14.3 ± 7.2	14.5 ± 9.8	9.0 ± 5.5	< 0.001	1.000	< 0.001	< 0.001
Right subclavian artery	19	16.5 ± 9.2	16.5 ± 10.3	10.1 ± 6.8	< 0.001	1.000	< 0.001	< 0.001
Left common carotid artery	48	9.2 ± 3.9	7.2 ± 4.5	6.4 ± 5.3	< 0.001	< 0.001	< 0.001	0.006
Right common carotid artery	50	8.7 ± 4.0	7.3 ± 4.9	6.3 ± 4.3	< 0.001	0.012	< 0.001	0.006

Data are mean ± standard deviation. The *P*-values for multiple pairwise comparisons were adjusted using Bonferroni method, and $P < 0.05$ indicates statistically significant difference.
CT = computed tomography, HIR = hybrid iterative reconstruction, DLR = deep learning reconstruction, HU = Hounsfield unit

https://doi.org/10.3348/kjr.2023.1078

the qualitative scores and quantitative parameters of the images. Notably, the Dark-blood-DLR approach demonstrated better consistency in wall thickness measurement.

The subtraction-based dark-blood CT method utilized in this study markedly enhanced the visualization of cervical artery walls by suppressing lumen density. Compared with Delayed-HIR, Dark-blood-HIR significantly increased the CNR of the vessel wall, particularly for the carotid arteries, with rate increments of 35.7% and 58.5%, respectively. Qualitative results also indicated that dark-blood CTA images provided higher scores in terms of vessel wall visualization and the diagnostic confidence index. Additionally, because of the integrated denoising filter, the dark-blood technique maintained image noise even with the subtraction and addition operations. Our method is an extension of the contrast-enhancement boost (CE-boost) technique, which has traditionally been utilized to further increase enhancement on contrast-enhanced CT for various body parts [19-21]. The CE-boost technique was modified to generate dark-blood CT images in which the paired arterial and delayed-phases served as inputs instead of the conventional pair of unenhanced and enhanced images. In this scenario, vessel wall enhancement and blood signal suppression were achieved by subtracting arterial-phase CT images from delayed-phase CT images. The subtracted images were then added to the original delayed-phase images using an automatic denoising procedure to generate the final dark-blood CT images. The proposed method can generate dark-blood images similar to those obtained using the dual-energy approach of Rotzinger et al. [7]. Their dual-energy CT material decomposition method improved the visualization of the aortic wall and intramural hematoma; however, only arterial-phase images were utilized to generate dark-blood images. In contrast, our study integrated both the arterial and delayed-phases of CTA images and contained additional inherent information on vascular wall enhancement physiologically occurring in the delayed-phase.

The dark-blood algorithm in our study is a software solution, and traditional triphasic head-neck CTA datasets are required as inputs, which can be easily integrated into the clinical workflow.

Recent studies have assessed the role of DLR in enhancing the image quality in head and neck CT imaging, including both non-enhanced cerebral CT [22] and the depiction of intracranial arteries in CTA [16]. Otgonbaatar et al. [16] demonstrated that DLR improved both the quantitative (average improvement of CNR of 44.8%) and qualitative performance in brain CTA images compared with HIR. In this study, we focused on the benefits of DLR for enhancing vascular wall visibility. We found that the CNR between the vascular wall and lumen obtained with Dark-blood-DLR increased by 26.4%–81.6% compared to Dark-blood-HIR, and by 77.2%–100% compared to Delayed-HIR. In terms of subjective image quality assessment, besides vessel wall visualization and diagnostic confidence index, Dark-blood-DLR also showed advantages in terms of overall image noise compared with Dark-blood-HIR. Our findings also indicated that, compared to traditional delayed-phase CTA images reconstructed with HIR, images with a combination of dark-blood and DLR showed remarkable improvement in both qualitative and quantitative image quality. The CNR between the vascular wall and lumen almost doubled, and the improvement in subjective scores indicated that a faster and more accurate diagnosis was achieved for thickened vessel walls.

The disease course of TAK is long, with varying degrees of activity. Previous studies have shown that vessel wall thickness in TAK serves as an indicator of disease activity and monitoring [6,23]. Our results demonstrated excellent inter-reader consistency of the Dark-blood-DLR in quantitative measurements of the carotid artery wall, surpassing the other two techniques. This indicates that Dark-blood-DLR CTA has the potential to become a useful quantitative tool for measuring vessel wall thickness with better accuracy and less variability. Further validation will be required in future studies.

Our study has several limitations. First, the sample size of this single-center study was relatively small and did not allow for a detailed analysis based on various disease conditions. Multicenter prospective trials are required to validate the clinical reliability and reproducibility of dark-blood CTA combined with DLR. Second, the method of delineating the ROI on the vessel wall was limited to vessel walls that ran vertically and exhibited a circular lumen on axial images. For vessels that are more tortuous or parallel in their paths on axial images, it may be possible to reconstruct images from other orientations for more accurate delineation. However, this was not attempted in the present study. Third, there is currently a lack of a gold standard reference for vessel wall thickness. Additionally, because of the limited amount of carotid artery wall MR data, we were unable to conduct a comparative study between CT and MR measurements of wall thickness. Therefore, further investigation is required for the clinical application of

https://doi.org/10.3348/kjr.2023.1078

Korean Journal of Radiology
KJR

Dark-blood-DLR CTA. Furthermore, future research should investigate clinical practices related to disease activity and follow-up evaluation of TAK, which was beyond the scope of the present study.

In conclusion, our study demonstrates that compared to Delayed-HIR, the dark-blood method combined with DLR can enhance the image quality of vessel wall CTA and improve the visualization of the cervical artery wall in patients with TAK. This enhancement is conducive to the rapid and accurate measurement of vessel wall thickness.

Availability of Data and Material

The datasets generated or analyzed during the study are available from the corresponding author on reasonable request.

Conflicts of Interest

Min Xu and Jian Wang is employee of Canon medical system (China) Co., Ltd. They had no control on the study raw data and analysis. The remaining author has declared no conflicts of interest.

Author Contributions

Data curation: Tong Su, Yu Chen. Funding acquisition: Yu Chen, Xinping Tian. Methodology: Tong Su, Zhe Zhang. Project administration: Jing Li. Resources: Yun Wang, Yumei Li. Software: Min Xu, Jian Wang. Supervision: Zhengyu Jin. Writing—original draft: Tong Su, Zhe Zhang. Writing—review & editing: Yu Chen, Xinping Tian.

ORCID IDs

Tong Su
https://orcid.org/0000-0002-4272-3130
Zhe Zhang
https://orcid.org/0009-0002-5810-1325
Yu Chen
https://orcid.org/0000-0001-9795-9311
Yun Wang
https://orcid.org/0000-0002-7495-5542
Yumei Li
https://orcid.org/0000-0003-3844-1912
Min Xu
https://orcid.org/0000-0001-5068-5632
Jian Wang
https://orcid.org/0000-0002-6179-3142
Jing Li
https://orcid.org/0000-0003-2504-1629
Xinping Tian
https://orcid.org/0000-0002-1511-7952
Zhengyu Jin
https://orcid.org/0000-0002-6179-9632

Funding Statement

This work was funded by the National Natural Science Foundation of China (grant number. 82001814) and the National High Level Hospital Clinical Research Funding (grant number. 2022-PUMCH-B-068).

REFERENCES

1. Seyahi E. Takayasu arteritis: an update. *Curr Opin Rheumatol* 2017;29:51-56
2. Park SH, Chung JW, Lee JW, Han MH, Park JH. Carotid artery involvement in Takayasu's arteritis: evaluation of the activity by ultrasonography. *J Ultrasound Med* 2001;20:371-378
3. Kerr GS, Hallahan CW, Giordano J, Leavitt RY, Fauci AS, Rottem M, et al. Takayasu arteritis. *Ann Intern Med* 1994;120:919-929
4. Park JH, Chung JW, Im JG, Kim SK, Park YB, Han MC. Takayasu arteritis: evaluation of mural changes in the aorta and pulmonary artery with CT angiography. *Radiology* 1995;196:89-93
5. Zhu FP, Luo S, Wang ZJ, Jin ZY, Zhang LJ, Lu GM. Takayasu arteritis: imaging spectrum at multidetector CT angiography. *Br J Radiol* 2012;85:e1282-e1292
6. Kim SY, Park JH, Chung JW, Kim HC, Lee W, So YH, et al. Follow-up CT evaluation of the mural changes in active Takayasu arteritis. *Korean J Radiol* 2007;8:286-294
7. Rotzinger DC, Si-Mohamed SA, Shapira N, Douek PC, Meuli RA, Boussel L. "Dark-blood" dual-energy computed tomography angiography for thoracic aortic wall imaging. *Eur Radiol* 2020;30:425-431
8. Rowe SP, Chu LC, Recht HS, Lin CT, Fishman EK. Black-blood cinematic rendering: a new method for cardiac CT intraluminal visualization. *J Cardiovasc Comput Tomogr* 2020;14:272-274
9. Mileto A, Guimaraes LS, McCollough CH, Fletcher JG, Yu L. State of the art in abdominal CT: the limits of iterative reconstruction algorithms. *Radiology* 2019;293:491-503
10. Brady SL, Trout AT, Somasundaram E, Anton CG, Li Y, Dillman JR. Improving image quality and reducing radiation dose for pediatric CT by using deep learning reconstruction. *Radiology* 2021;298:180-188
11. Xu C, Xu M, Yan J, Li YY, Yi Y, Guo YB, et al. The impact of deep learning reconstruction on image quality and coronary CT angiography-derived fractional flow reserve values. *Eur Radiol* 2022;32:7918-7926
12. Otgonbaatar C, Jeon PH, Ryu JK, Shim H, Jeon SH, Ko SM, et al. Coronary artery calcium quantification: comparison between filtered-back projection, hybrid iterative reconstruction, and deep learning reconstruction techniques. *Acta Radiol* 2023;64:2393-2400

13. Otgonbaatar C, Ryu JK, Shin J, Kim HM, Seo JW, Shim H, et al. Deep learning reconstruction allows for usage of contrast agent of lower concentration for coronary CTA than filtered back projection and hybrid iterative reconstruction. *Acta Radiol* 2023;64:1007-1017
14. Otgonbaatar C, Ryu JK, Shin J, Woo JY, Seo JW, Shim H, et al. Improvement in image quality and visibility of coronary arteries, stents, and valve structures on CT angiography by deep learning reconstruction. *Korean J Radiol* 2022;23:1044-1054
15. Sato M, Ichikawa Y, Domae K, Yoshikawa K, Kanii Y, Yamazaki A, et al. Deep learning image reconstruction for improving image quality of contrast-enhanced dual-energy CT in abdomen. *Eur Radiol* 2022;32:5499-5507
16. Otgonbaatar C, Ryu JK, Kim S, Seo JW, Shim H, Hwang DH. Improvement of depiction of the intracranial arteries on brain CT angiography using deep learning reconstruction. *J Integr Neurosci* 2021;20:967-976
17. Wang Y, Chen Y, Liu P, Lv W, Wu J, Wei M, et al. Clinical effectiveness of contrast medium injection protocols for 80-kV coronary and craniocervical CT angiography-a prospective multicenter observational study. *Eur Radiol* 2022;32:3808-3818
18. Canon Medical Systems. White paper: advanced intelligent clear-IQ engine (AiCE) deep learning reconstruction: whole organ coverage with extraordinary image quality at the fast pace of medicine [accessed on March 12, 2024]. Available at: https://global.medical.canon/publication
19. Iizuka H, Yokota Y, Kidoh M, Oda S, Ikeda O, Tamura Y, et al. Contrast enhancement boost technique at aortic computed tomography angiography: added value for the evaluation of type II endoleaks after endovascular aortic aneurysm repair. *Acad Radiol* 2019;26:1435-1440
20. Otgonbaatar C, Jeon PH, Ryu JK, Shim H, Jeon SH, Ko SM, et al. The effectiveness of post-processing head and neck CT angiography using contrast enhancement boost technique. *PLoS One* 2023;18:e0284793
21. Otgonbaatar C, Ryu JK, Shim H, Jeon PH, Jeon SH, Kim JW, et al. A novel computed tomography image reconstruction for improving visualization of pulmonary vasculature: comparison between preprocessing and postprocessing images using a contrast enhancement boost technique. *J Comput Assist Tomogr* 2022;46:729-734
22. Oostveen LJ, Meijer FJA, de Lange F, Smit EJ, Pegge SA, Steens SCA, et al. Deep learning-based reconstruction may improve non-contrast cerebral CT imaging compared to other current reconstruction algorithms. *Eur Radiol* 2021;31:5498-5506
23. Chen B, Wang X, Yin W, Gao Y, Hou Z, An Y, et al. Assessment of disease activity in Takayasu arteritis: a quantitative study with computed tomography angiography. *Int J Cardiol* 2019;289:144-149

https://doi.org/10.3348/kjr.2023.1078